

Figure 6 Measured peak antenna gain and radiation efficiency for the two antennas studied in Figure 3(a). [Color figure can be viewed in the online issue, which is available at www.interscience.wiley.com]

behavior in both resonant modes is seen from the simulation results (not shown here for brevity) to rapidly deteriorate by about 10 dB.

Figures 4 and 5 give the far-field, 2-D radiation patterns in E_θ and E_ϕ fields at 2442 and 5490 MHz, the center operating frequencies of the 2.4 and 5 GHz bands. Other frequencies in the bands of interest were also measured, and no appreciable difference in radiation patterns was obtained. It is easy to see that good omni-directional radiation patterns in the horizontal plane (that's the x - y plane here) are obtained from the test results. Notice that though the monopole antenna is utilized for 2.4 GHz operation, the antenna system (radiating strip and ground plane thereof) can radiate a dipole-like radiation pattern. This is because both the radiating strip and the ground plane are of quarter-wavelength resonant structure with no null surface currents occurring in both portions at the same operating frequency.

Figure 6 plots the measured peak antenna gain and radiation efficiency. The peak-gain level in the 2.4 GHz band is about 2.1 dBi; the radiation efficiency exceeds about 83%. As for the 5.2 GHz band, the peak gain is in the range of 2.6–3.1 dBi with radiation efficiency larger than 79%. Notice that the radiation efficiency was obtained in the 3-D test system by calculating the total radiated power of an antenna under test (AUT) over the 3-D spherical radiation first and then dividing the total amount by the input power (default value is 0 dBm) given to the AUT.

4. CONCLUSION

A two-antenna system formed by arranging a monopole antenna and a dipole antenna both printed on a dielectric substrate for concurrent, WLAN AP applications has been demonstrated, studied, and tested. The results show that though the distance between the two WLAN antennas is 1 mm, good isolation of less than -20 dB over the 2.4 and 5 GHz bands is still obtained. In addition, dipole-like radiation patterns with good omni-directional radiation in the horizontal plane have been observed. Peak antenna gain is about 2.1 and 2.9 dBi for the 2.4 and 5 GHz antennas, respectively. The proposed design is well suited for concurrent 2.4 and 5 GHz band operation in an access point, which does not lose extra gain when compared with the case of a single-feed, dual-band access point using an external diplexer for concurrent operation.

REFERENCES

1. S.W. Su, Y.T. Chen, and K.L. Wong, Printed dual-band U-slotted monopole antenna for WLAN access point, *Microwave Opt Technol Lett* 38 (2003), 436–439.

2. K.L. Wong, J.W. Lai, and F.R. Hsiao, Omnidirectional planar dipole-array antenna for 2.4/5.2-GHz WLAN access points, *Microwave Opt Technol Lett* 39 (2003), 33–36.
3. K.M. Luk and S.H. Wong, A printed high-gain monopole antenna for indoor wireless LANs, *Microwave Opt Technol Lett* 41 (2004), 177–180.
4. F.R. Hsiao and K.L. Wong, Omnidirectional planar folded dipole antenna, *IEEE Trans Antennas Propag* 52 (2004), 1898–1902.
5. R. Bancroft, Design parameters of an omnidirectional planar microstrip antenna, *Microwave Opt Technol Lett* 47 (2005), 414–418.
6. S.W. Su and J.H. Chou, Printed omnidirectional access-point antenna for 2.4/5-GHz WLAN operation, *Microwave Opt Technol Lett* 50 (2008), 2403–2407.
7. K.L. Wong and J.H. Chou, Integrated 2.4- and 5-GHz WLAN antennas with two isolated feeds for dual-module applications, *Microwave Opt Technol Lett* 47 (2005), 263–265.
8. S.W. Su, J.H. Chou, and Y.-T. Liu, Printed coplanar two-antenna element for 2.4/5 GHz WLAN operation in a MIMO system, *Microwave Opt Technol Lett* 50 (2008), 1635–1638.

© 2009 Wiley Periodicals, Inc.

RESONANCE TRANSMISSION THROUGH ELECTROMAGNETIC CRYSTALS CONSISTING OF METAL STRIPS

Ruey Bing Hwang

Department of Communication Engineering, National Chiao Tung University, Hsinchu, Taiwan, Republic of China; Corresponding author: raybeam@mail.nctu.edu.tw

Received 4 September 2008

ABSTRACT: In this letter, we present frequency-selective transmission of a 2D (two-dimensionally) electromagnetic (EM) crystal. Such a 2D EM crystal consists of a finite stack of one-dimensionally metal-strip gratings. The rigorous mathematical formulation using the mode-matching method incorporating the Floquet solution was employed to calculate the scattering and guiding characteristics of the structure under consideration. Additionally, the experimental studies were also carried out to verify the numerical results. Significantly, the correlation between frequency-selective transmission and the Fabry-Perot resonance was clarified. © 2009 Wiley Periodicals, Inc. *Microwave Opt Technol Lett* 51: 1209–1212, 2009; Published online in Wiley InterScience (www.interscience.wiley.com). DOI 10.1002/mop.24280

Key words: two-dimensionally periodic structures; electromagnetic crystals; electromagnetic band-gap structures

1. INTRODUCTION

The frequency selective surface (FSS) has been extensively studied for many years. A typical FSS is a one-dimensionally (1D) or two-dimensionally (2D) periodic structure with the unit cell made up of thin conducting elements printed on a dielectric substrate for supporting [1–6]. In addition to the single-layer FSS, a cascade of metal-strip gratings has been developed [5, 6]. In [5], the researchers considered each individual metal-strip grating as a FSS and synthesize the desired final behavior as a cascade of FSSs. On the other hand, an alternative approach based on a “guided” viewpoint instead of “diffraction” was proposed [6].

Although the guided wave concept was proposed, the detail mathematical formulation and guided wave phenomena; such as the dispersion relation of the multilayer FSS were not tackled. In this letter, we study the transmission characteristic of a 2D elec-

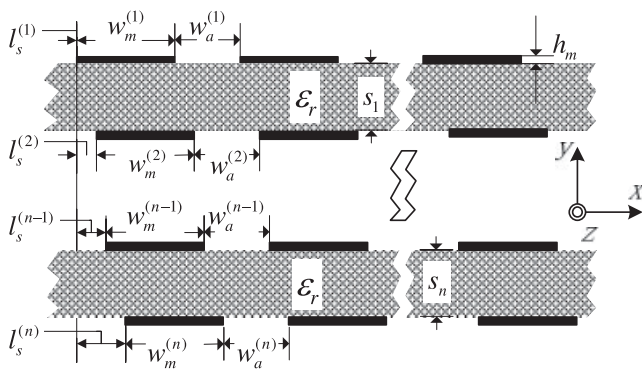


Figure 1 Structural configuration and geometric parameters assignment of a 2D EM crystal

tromagnetic (EM) crystal containing multilayer metal-strip gratings. The rigorous mode-matching method incorporating the Floquet solution was employed to calculate the scattering- and guiding- characteristic. Additionally, experimental studies for measuring the transmittance of EM crystals were also carried out. The good agreement between the measured and calculated results was achieved. Last but not least, the resonance transmission frequency was carefully identified by the Fabry-Perot resonance obtained by evaluating the dispersion relation of the EM crystal.

2. STATEMENT OF THE PROBLEM

Figure 1 shows a 2D EM crystal comprised of metal strips. In effect, such a structure can be regarded as a finite stack of 1D metal gratings. With respect to the rectangular coordinate system attached, the metal grating is assumed to be infinite in extent along the z direction. Moreover, the number of period along the x direction is also supposed to be infinity. Each of metal strips has the width w_m and thickness h_m , and the separation distance between two strips is w_a . Thus, the period of the metal strip array along the x direction (dx) is $w_m + w_a$. Notably, the metal strip considered here is assumed to be a perfect conductor; namely, electric field is zero therein. Returning to Figure 1, a uniform dielectric layer serving as a separator has the relative dielectric constant ϵ_r , and thickness s . Furthermore, each of 1D metal-strip gratings may have the shift distance l_s in lateral direction (along the x axis); the parameter l_s in each layer could be properly chosen to synthesize a lattice pattern, such as a square- or triangular-lattice. Regarding the excitation, a uniform plane wave is normally incident into this structure. The incident plane wave with electric field vector along the z direction will hereafter be termed as TE polarization, while TM polarization having magnetic field vector along the z direction.

3. METHOD OF ANALYSIS

As mentioned earlier, a 2D EM crystal can be regarded as a finite stack of 1D metal-strip gratings. Therefore, the scattering characteristic of a 2D EM crystal can be treated as a cascade of that of the 1D metal grating. Once the input-output relation of a 1D metal grating is determined, the scattering characteristic of the multilayer metal gratings can be readily obtained by subsequently employing the input-output relation and transfer matrix of the metal grating [7]. Such a method was termed the building block approach, which is intensively employed in microwave engineering.

Since the metal strip was supposed to be made by perfect metal, the electric field inside metal strip vanishes. On the other hand, the region between two metal strips is a parallel-plate waveguide, so

that the electric- and magnetic- field can be expressed in terms of the superposition of parallel-plate waveguide modes. Outside the metal grating; namely, in a uniform dielectric medium, the electric- and magnetic- field are expressed in terms of the Floquet (or plane wave) solution. After matching the EM boundary condition; that is, the tangential electric- and magnetic- field must be continuous across the interface between metal grating and uniform medium. In doing so, we can obtain the input-output relation at the interface with discontinuities. Moreover, after some mathematical formulation, the input-output relation of the 1D metal grating can be achieved. By cascading the input-output relation of each 1D metal grating, the scattering characteristics, including reflectance and transmittance, of the overall structure are determined. Since the detail mathematical formulation was reported in literature [7], we would not repeat the complex mathematical procedure for the succinctness of this letter.

4. PROCEDURE OF MEASUREMENT

In this section, we present a set-up for measuring the transmission characteristics of an EM crystal. This measurement system consists of a vector network analyzer, microwave power amplifiers, coaxial cables, broad-band standard horn antennas, and foam absorbers. The 2D EM crystal is sandwiched between two masks made from foam absorber. Due to the theoretical model described in previous section, the structure and field are assumed to have no variation along the length direction of the metal grating. Therefore, the diffraction from edges of the EM crystal is eliminated by putting masks on the 2D EM crystal for shielding the edge of the structure under test, where the mask is made by carving out a rectangular aperture from a microwave absorber. Notably, the area under illuminating should cover enough numbers of periods for preserving the characteristic of periodic structures. There are 20 periods that are visual from the mask. Moreover, such a mask can maintain almost uniform field strength over the aperture and the EM crystal, as well. However, due to the Gaussian beam radiating from the horn antenna instead of an ideal plane wave, phase difference over the aperture shall cause a slight difference between the theoretical and measured results.

5. THEORETICAL AND MEASURED RESULTS

We have implemented two types of 1D metal-strip grating with metal strip width 10 mm and 15 mm, respectively, while they share the same period along the x direction, which is 20 mm. The metal strip is made of copper foil with the thickness $h_m = 0.06$ mm. These metal strips were coated on a dielectric layer (Polystyrene) having the relative dielectric constant close to unity. Once the 1D metal gratings are fabricated, the 2D EM crystal could be readily implemented by stacking them up.

In the first example, we demonstrated transmission characteristics of a structure containing two 1D metal-strip gratings. The metal-strip width and period along the x direction are 15 mm and 20 mm, respectively. The separation distance between two 1D metal-strip gratings is 24 mm. Additionally, the lateral shift distance between two 1D metal-strip gratings is zero. Figure 2 shows the variation of transmittance against frequency for both measurement and calculation. As shown in this figure, the theoretical calculation depicts two transmission peaks around 6 GHz and 12 GHz, respectively. Since each of the transmission peaks has a large quality factor, they may be caused by the resonance effect of the structure under consideration.

To investigate the physical consequences of resonance transmission, we carry out the calculation of the dispersion relation of guided waves supported in the structure shown in the inset of

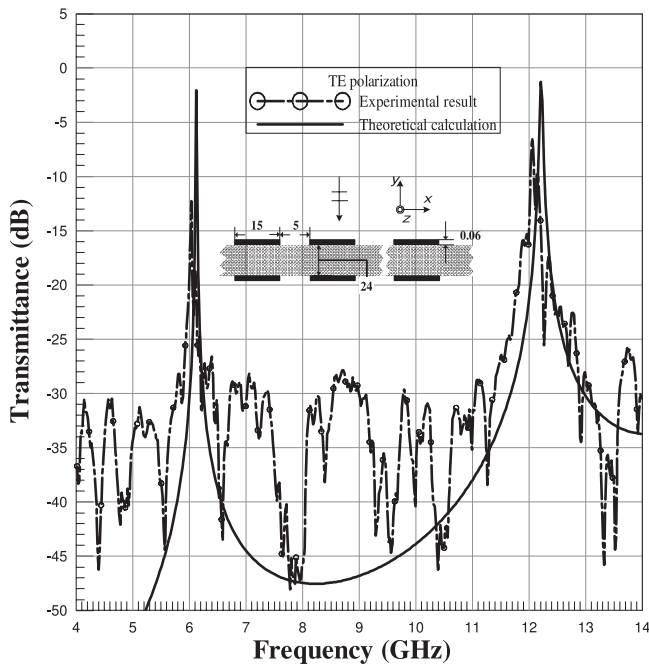


Figure 2 Variation of transmittance against frequency for both measured and calculated results; TE polarized incident wave.

Figure 2. Figure 3 demonstrates the distribution of normalized phase constant along the x -direction ($\beta_x d/2\pi$) versus frequency. As was reported in [8], the resonance (frequency-selective) transmission is due to the phase-matching between the incident plane wave and the wave guided in a leaky waveguide. Thus, the dispersion relation of waveguide allows us to determine resonance transmission frequencies of the incident plane wave. For a plane wave with normal incidence, we can read resonance frequencies from the intersection points of the dispersion curve and the vertical axis; which are 6.076 GHz and 12.103 GHz, respectively.

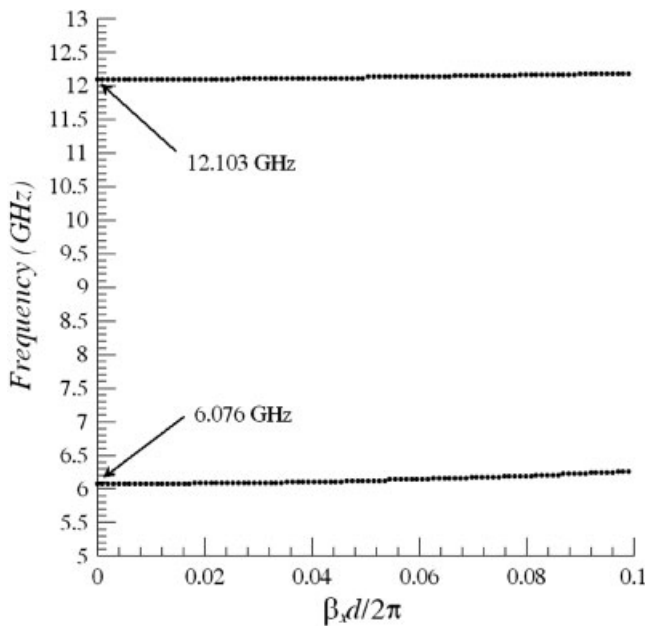


Figure 3 Dispersion relation of guided wave in the waveguide consisting of two 1D metal-strip arrays shown in the inset of Figure 2.

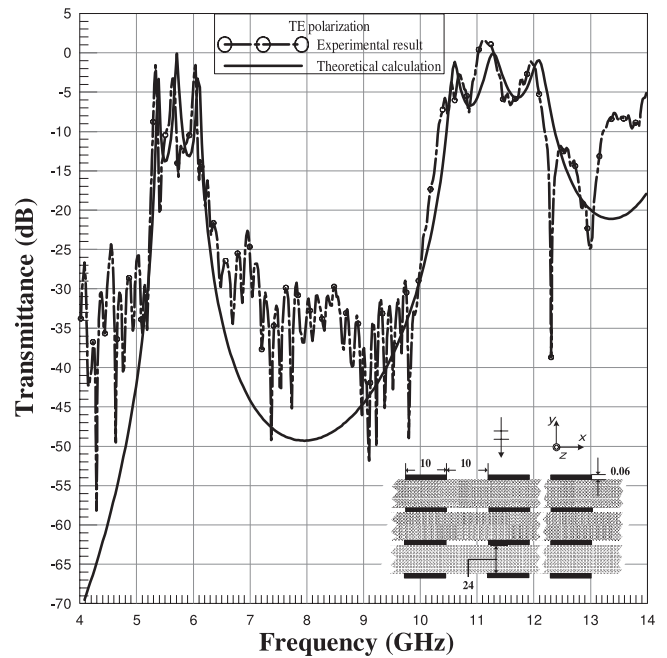


Figure 4 Variation of transmittance against frequency for both experimental measurement and theoretical calculations; TE plane wave incidence.

In the next example, we increase the number of 1D metal-strip grating up to 4, while the metal-strip width decreases to 10 mm. As indicated in Figure 4, there are two pass bands having broad bandwidth than those shown in Figure 2. Different from the result in Figure 2, each of the pass bands has three transmission peaks. In effect, the transmission peak is also contributed by the Fabry-Perot resonance. The structure contains four 1D metal gratings; meanwhile, they form three resonators. Since those resonators are not isolated, they couple to one another through slits of the metal-strip grating. Although all resonators share the same structure param-

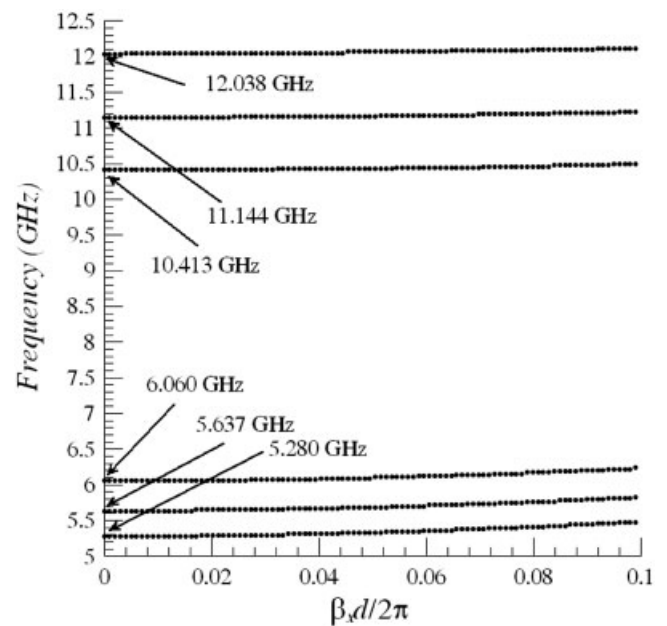


Figure 5 Dispersion relation of guided wave in the waveguide consisting of four 1D metal-strip arrays shown in the inset of Figure 4.

ters, the coupling effect leads to the separation for resonance frequencies, as depicted in Figure 4.

To again prove the correlation between the resonance transmission and the Fabry-Perot resonance, we calculate the dispersion relation of the wave-guiding structure shown in the inset of Figure 4. It is apparent to see that each of peak frequencies respectively corresponds to the Fabry-Perot resonance frequency, as was obtained by the dispersion relation of the 4-layer metal grating structure. The six peak frequencies are pointed out in Figure 5.

6. CONCLUSION

In this letter, a frequency-selective transmission structure consisting of 2D metal-strip gratings was thoroughly investigated. The resonance transmission due to the Fabry-Perot resonance underlying a 2D EM crystal was demonstrated experimentally and theoretically. Significantly, the resonance frequencies were accurately predicted by the Fabry-Perot resonance frequencies obtained by carrying out the calculation of the dispersion relation of a 2D EM crystal.

ACKNOWLEDGMENTS

This author thanks Thang Dong Hwang for implementing 2D EM crystals. This work was supported in part by the National Science Council, Taiwan, R.O.C. under the contract number 95–2221-E-009–045-MY3.

REFERENCES

1. B.A. Munk, *Frequency selective surface: Theory and design*, Wiley, New York, 2000.
2. B.A. Munk, *Finite antennas arrays and FSS*, Wiley, New York, 2000.
3. C.V. John, *Frequency selective surfaces*, U. K. Research Tuddies Press, 1997.
4. T.K. Wu, *Frequency selective surfaces and grid array*, Wiley, New York, 1995.
5. P.W.B. Au, E.A. Parker, and R.J. Langley, Wide band filters employing multilayer gratings, *IEE Proc H* 140 (1993), 292–296.
6. D. Kinowski, M. Guglielmi, and A.G. Roederer, Angular bandpass filters: An alternative viewpoint gives improved design flexibility, *IEEE Trans Antennas Propag* 43 (1995), 390–395.
7. R.B. Hwang, Relation between the reflectance and band structure of 2-D metalodielectric electromagnetic crystals, *IEEE Trans Antennas Propag* 52 (2004), 1454–1464.
8. R.B. Hwang and C.C. Hsiao, Frequency-selective transmission by a leaky parallel-plate-like waveguide, *IEEE Trans Antennas Propag* 54 (2006), 121–129.

© 2009 Wiley Periodicals, Inc.

SCM TRANSMISSION IN MM FIBER WITH AUTOMATIC SELECTION OF THE SUBCARRIER FREQUENCY

Marcin Kowalczyk and Jerzy Siuzdak

Instytut Telekomunikacji Politechniki Warszawskiej, 00-665 Warszawa, ul. Nowowiejska 15/19, Poland; Corresponding author: siuzdak@tele.pw.edu.pl

Received 11 September 2008

ABSTRACT: Demonstrated was a 10 Mbit/s binary frequency shift keying subcarrier multiplexing system operating beyond the pass-band of 1 km MM graded index optical fiber. The system automatically adjusted the carrier frequency to the fiber frequency response. Transmission of four 10 Mbit/s channels was also shown over the same fiber. No visible

channel interaction was observed. © 2009 Wiley Periodicals, Inc. *Microwave Opt Technol Lett* 51: 1212–1214, 2009; Published online in Wiley InterScience (www.interscience.wiley.com). DOI 10.1002/mop.24277

Key words: multimode fiber; data transmission; subcarrier multiplexing; modulation; frequency shift keying

1. INTRODUCTION

It is well known that contemporary graded index (GI) SiO₂ optical fibers exhibit frequency ranges beyond the base-band that are suitable for transmission [1–3]. Several systems have been built that made use of this fact [1, 3–6]. They employed subcarrier multiplexing (SCM), where one or more subcarriers were located in appropriate frequency regions outside the base-band and modulated with transmitted data. However, as the MM fiber passband frequency response is almost impossible to determine a priori, the exact location(s) of subcarrier(s) had to be selected manually based on the (frequency response) measurements. Furthermore, the systems realized so far usually shared the same carrier oscillator between transmitter and receiver, which is obviously not suitable for any practical operation [1, 3–6]. Here, we present a system that automatically selects subcarrier frequency, and moreover its receiver is separated from the transmitter.

2. SYSTEM DESCRIPTION

A block scheme of the realized SCM system is shown in Figure 1 and its photograph in Figure 2. The system used binary frequency shift keying (BFSK) with the 10 Mbit/s bit rate produced by pseudorandom bit sequence (PRBS) generator. This type of modulation was chosen because of relative simplicity and resistance to nonlinear distortions in multichannel environment. Apart from the obvious fiber link both the transmitter and receiver were connected the LPT port of a personal computer (PC). At the transmitter, the central frequency of the oscillator (voltage controlled oscillator, VCO) was set externally from the LPT port. The VCO instantaneous frequency could be also modulated by PRBS data. The signal originating from the oscillator drove a VCSEL laser operating at 850 nm. After propagation along the fiber, the optical signal was converted back to electrical domain and underwent typical heterodyne frequency demodulation. First, it was converted to a 69 MHz intermediate frequency and then divided two ways with 0° and 90° phases (see Fig. 1). In 90° branch, there was an additional frequency sensitive phase shifter that converted frequency modulation to phase modulation. The latter was detected by a phase detector and visualized by an oscilloscope. Both the transmitter and receiver were made with typical off-shelf RF devices.

The system operated in two steps. At the initialization stage, the BFSK was switched off and the frequency response of the fiber was measured over the useful frequency range (520–1040 MHz in this case). It was performed changing step by step the frequency of the VCO at the transmitter, and measuring the respective value of the signal power at the receiver.

The latter was fed to the PC via the LPT port. The initialization stage ended with the automatic selection of carrier frequency at a frequency region suitable for transmission (i.e., relatively low attenuation and flat characteristic over sufficient frequency range). In any practical system, however, the initialization stage would require a feedback channel be established between receiver and transmitter.

During the normal operation (second stage) the carrier is set and BFSK modulation is switched on.